Microscopic characterization of overpressurized superfluid ^{4}He

M. Rossi

Dipartimento di Matematica, Politecnico di Milano, Piazza Leonardo da Vinci 32, IT-20133 Milano, Italy

E. Vitali, L. Reatto, and D. E. Galli

Dipartimento di Fisica, Università degli Studi di Milano, via Celoria 16, IT-20133 Milano, Italy

We have studied static and dynamical properties of superfluid ^{4}He at $T = 0$ K in the pressure range from -6 up to 87 atm well above freezing into the metastable region. Zero temperature properties have been obtained with the *exact* shadow path integral ground state (SPIGS) method. Information about dynamic structure factors at different pressures have been obtained from imaginary time correlation functions via the genetic inversion via falsification of theories (GIFT) method. In the full pressure range sharp roton excitations are always present in the spectral functions. The roton energy decreases at higher pressures in good agreement with experimental data also in the metastable region. The roton energies have essentially a linear trend with pressure, going from about 7.4 K near freezing to about 4.3 K at about 87 atm. The pressure at which the linear trend would extrapolate to a zero roton energy turns out to be about 170 atm. At $T = 0$ K, no sign of metastable glass phase has been found; the disordered systems studied at pressures above about 87 atm readily start homogeneous nucleation processes. Our results in the metastable phase for the condensate fractions and roton gaps differ remarkably from previous ones obtained via a diffusion Monte Carlo study.

I. INTRODUCTION

First-order phase transitions are characterized by discontinuities in some physical properties of many-body systems: the free-energy landscape offers the conditions of the spontaneous emergence of a new phase. Typically, a free-energy barrier has to be overcome to realize the nucleation of the new phase, giving rise to interesting metastability phenomena. In this work we focus on the ^{4}He superfluid-solid transition. Such a transition is particularly interesting in connection with the hot topic of supersolidity, where metastable states have been invoked as a possible explanation for the intriguing experimental findings.[1]

Several theoretical studies have suggested that excitations modes are closely related to intrinsic instability of the liquid phase.[2,3] In a theory of the superfluid-solid transition[4] of ^{4}He it was recognized that the superfluid phase becomes intrinsically unstable against a density fluctuation at a wave vector corresponding to the roton excitation. It is thus very interesting to investigate the fate at high density of the phonon-roton spectrum. Experimental studies have recently shown that it is indeed possible to pressurize liquid ^{4}He well above the freezing point, both in bulk systems via acoustic techniques[5–7] and, in a more restricted range, in porous media where neutron scattering experiments have been carried out.[8]

In literature there are few *ab initio* quantum Monte Carlo (QMC) studies of overpressurized liquid ^{4}He.[9–11] Two of these were devoted to compute mainly off-diagonal properties with path integral QMC methods at zero[9] and finite[11] temperature. Only in were Ref. 10 excited state properties computed; such a study used the released node diffusion Monte Carlo (RN-DMC) technique. The excited state results were affected by quite large statistical uncertainties, somehow obscuring the interpretation; the roton gap did not seem to extrapolate to zero and this could influence the physical picture of the homogeneous nucleation in this system.

The simulation of metastable phases is a delicate issue since in general simulation methods, when convergence is achieved, sample configurations of the equilibrium state and the metastable state represents only a transient. But this is true also for metastable phases in nature: the key point is whether a transient in Monte Carlo dynamics could provide a realistic description of what actually happens in the physical system. Only a comparison with experiments can tell us whether the imaginary time dynamics of a particular method is capturing the actual physical behavior of the metastable system. We argue that the best one can do is to let only the Hamiltonian operator play a role, without any constraint forcing a particular phase. Path integral calculations, at finite and zero temperature, are thus very suitable for our aim since only $e^{-s\hat{H}}$ governs the imaginary time propagation, $\hat{H}$ representing the Hamiltonian operator of the system.

II. METHODOLOGY

In this work we address an *ab initio* QMC study of the excitation spectrum of liquid ^{4}He under pressure at $T = 0$ K using the *exact* shadow path integral ground state method (SPIGS).[12–14] The SPIGS method is a path integral ground state (PIGS) method[15] that projects a shadow wave function[16] ψ_{sh}. We have checked that another choice of the starting wave function, a Jastrow wave function, leads to the same results within statistical errors up to the highest considered densities in the overpressurized region. So, as we will discuss below, the metastable phase with SPIGS arises simply from the initial conditions, similar to what happens in a real metastable phase. With SPIGS the only approximations regard the short time propagator $\langle \mathcal{R} | e^{-\frac{s}{M}\hat{H}} | \mathcal{R}' \rangle$ with $M \gg 1$, and the fixed total projection time s, but it is possible to reduce the systematic errors under the statistical noise level. We have used both the pair-product[17] and the pair-Suzuki[14] approximations for the propagator; in the first case the imaginary time step was chosen
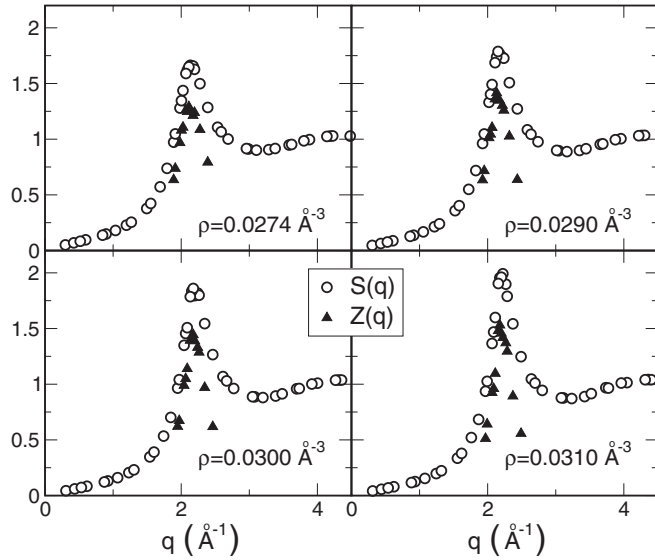
FIG. 1. (Circles) Static structure factor $S(q)$ and (triangles) strength of the single quasiparticle peak $Z(q)$ for different densities above freezing. Statistical uncertainties are below the symbol size.

to be $s/M = 1/160$ K^{-1}, while for the second approximation we used $s/M = 1/320$ K^{-1}. Typical total projection time was of the order of 0.5 K^{-1}. Finally, the excitation spectrum can be in principle extracted from imaginary time correlation functions without relying on any approximation paying the fee of facing an ill-posed inverse problem. We have recently developed a technique to face such problems, the genetic inversion via falsification of theories (GIFT) strategy.[18] When applied to stable liquid ^{4}He at $T = 0$ K, GIFT has been shown to be very accurate, recovering spectral functions with sharp quasiparticle excitations displaying also the multiphonon branch. As a pair interaction potential among ^{4}He atoms we used two different parametrizations of the Aziz potential;[19,20] for comparison with the RN-DMC results we show here mainly the results obtained with the potential in Ref. [19].

III. RESULTS

The metastable phase turned out to be accessible for pressures up to $P_{max} \simeq 87$ atm, that is, for densities up to 0.031 Å^{-3}; at higher densities the system starts homogeneous nucleation processes within few thousand Monte Carlo (MC) steps. Nevertheless, below and at 87 atm we have been able to evaluate the excitation spectrum and the condensate fraction, for which recent accurate measurements near the freezing point are available.[21] We proceeded in the following way: for each studied density, we equilibrated a liquid-like configuration, suitably rescaled in density; after equilibration, the disordered phase was found persistent, with no sign of crystallization as inferred from the static structure factor $S(\vec{q}) \propto \langle \psi_0 | \hat{\rho}_{\vec{q}} \, \hat{\rho}_{-\vec{q}} | \psi_0 \rangle$ (see Fig. 1), $\hat{\rho}_{\vec{q}}$ being the Fourier component of the local density operator, allowing us to perform measurements on the metastable phase. Only for the highest density reported, $\rho = 0.0310$ Å^{-3}, after runs of many hundreds of thousand of MC steps, signs of partial crystallization have been detected in $S(\vec{q})$: out of many MC histories a few of the replicas display a growing Bragg peak during the MC evolution. We have
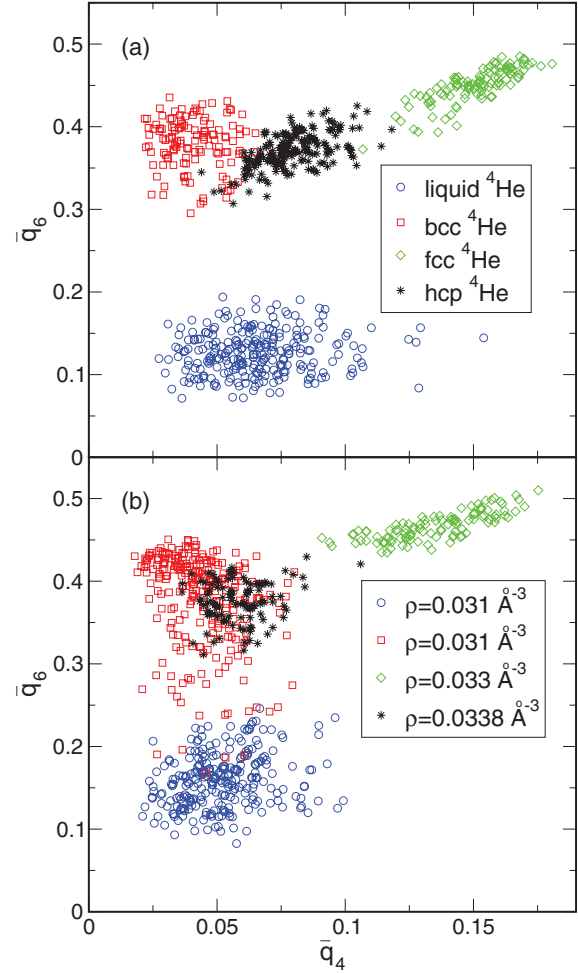

FIG. 2. (Color online) (a) $\bar{q}_4$-$\bar{q}_6$ values obtained for ^{4}He in liquid at $\rho = 0.0218$ Å^{-3} and in solid at $\rho = 0.029$ Å^{-3} for three different perfect crystals. (b) $\bar{q}_4$-$\bar{q}_6$ values obtained for the final configuration of ^{4}He systems simulated at different densities above melting starting from a disordered configuration.

also obtained the same conclusions by monitoring the so called *averaged local bond parameter* in the $\bar{q}_4$-$\bar{q}_6$ plane.[22] In Fig. 2(a) we show the typical signals obtained by analyzing a configuration explored by simulating ^{4}He hcp, fcc, and bcc perfect crystals compared with a typical liquid result. The important point is that, starting from disordered configurations to simulate the metastable phase, we always found liquid like spots up to $\rho = 0.031$ Å^{-3} [circles in Fig. 2(b)]; after very long runs at $\rho = 0.031$ Å^{-3} the system can be found in a (defected) solid-like configuration [squares in Fig. 2(b)]; at higher densities the systems readily starts a nucleation process [stars and diamonds in Fig. 2(b)].

All the results shown here have been obtained with systems of $N = 256$ ^{4}He atoms in periodic boundary conditions. Our results for the energy per particle and the pressure are reported in Table I. The pressure has been computed directly during the simulation via a virial estimator.[23] P_{vir} is in good agreement with the pressures inferred via a polynomial fit of the equation of state:

$$E(\rho) = E_0 + a(\rho/\rho_0 - 1)^2 + b(\rho/\rho_0 - 1)^3 \tag{1}$$

TABLE I. Energy per particle E/N and pressure computed with the virial estimator P_{vir}; the estimated condensate fraction n_0 and the parameters of the parabolic fit to the spectrum in the roton region Δ_R, q_R, and μ_R are also shown.

ρ (Å^{-3})	E/N (K)	P_{vir} (atm)	n_0	Δ_R (K)	q_R (Å^{-1})	μ_R/m_4
0.0200	−7.236(5)	−6.1(1)	0.117(6)	9.26(10)	1.844(13)	0.195(42)
0.0210	−7.325(4)	−3.7(1)	0.086(6)	9.03(8)	1.893(7)	0.140(16)
0.0218	−7.344(5)	−1.3(1)	0.069(4)	8.78(8)	1.908(6)	0.124(13)
0.0240	−7.241(4)	9.04(5)	0.043(4)	8.29(11)	1.978(7)	0.105(12)
0.0250	−7.093(5)	15.5(1)	0.036(4)	7.87(13)	2.026(9)	0.128(20)
0.0260	−6.875(7)	23.6(1)	0.025(2)	7.52(9)	2.048(6)	0.118(12)
0.0274	−6.447(7)	37.2(1)	0.017(2)	6.83(14)	2.089(8)	0.104(14)
0.0290	−5.768(4)	56.2(2)	0.010(2)	5.79(13)	2.139(7)	0.087(9)
0.0300	−5.227(5)	70.4(2)	0.0054(9)	5.13(10)	2.182(6)	0.090(7)
0.0310	−4.611(5)	86.7(1)	0.0036(9)	4.30(22)	2.206(13)	0.092(16)

with $E_0 = -7.352(2)$ K, $a = 13.74(26)$ K, $b = 7.44(47)$ K, and $\rho_0 = 0.02207(2)$ Å^{-3}. The energy turns out to be below experimental data suggesting, as is well known, that the interaction in Ref. [19] needs the inclusion of three-body contributions in $\hat{H}$ to compare with experiments, contrary to the effective two-body potential in Ref. [20]. Our results for the total energy per particle differ from those obtained with DMC[10,24] by many standard deviations at all considered densities. This is really unexpected in comparing two *exact* QMC methods. We have checked our results with three independent PIGS codes always obtaining compatible energies to those reported in Table I. We have also compared the energy of the system at equilibrium density with a DMC calculation (S. Moroni, private communications) which confirms our ground state result. We note this problem only with the energy results obtained in Refs. [10] and [24] with the interaction in Ref. [19] and the origin of such disagreement is still unknown; on the contrary, substantial agreement between our results and those in Ref. [24] or other DMC calculations[25] is present when the older interaction[20] is considered. Moreover, this difference grows significantly in the metastable region giving rise to big differences in the estimated equations of state; for example, at $\rho = 0.031$ Å^{-3} the DMC equation of state gives a pressure of about 25 atm above our result. The equation of state obtained from the older potential[20] [with fit parameters $E_0 = -7.162(3)$ K, $a = 14.57(47)$ K, $b = 5.01(68)$ K, and $\rho_0 = 0.02193(4)$ Å^{-3}] turns out to be in better agreement with experimental data (see Refs. [26] and [27]) contrary to what was found in Refs. [24] and [10] (see Fig. 3). The discrepancies of our pressures with respect to experimental data are of the order of 1 atm when using the newer potential[19] while it is reduced to about 0.3 atm with the older potential.[20] Remarkably extrapolated SPIGS results for pressure are in reasonable agreement with experimental data extrapolated in the overpressurized region,[27] up to densities of about 0.035 Å^{-3}.

In Table I we report also results for the condensate fraction n_0 obtained with a worm-like algorithm[28] implemented with SPIGS; this gives access also to the off-diagonal properties during a single simulation run at a fixed number of particles. Our results for the condensate fraction n_0 are in agreement with previous zero temperature reptation MC results[9] in the density range [0.0219–0.0293] Å^{-3} and with finite temperature results[11] at $\rho = 0.0292$ Å^{-3}. In Fig. 4 our results for n_0 are compared with the DMC ones[10]; large discrepancies are present between the two results; we recall however that DMC

calculations of n_0 do not rely on pure estimators and thus do not represent *exact* calculations of n_0. A recent path integral ground state calculation of n_0 is compatible with the results we found[29] in the density range considered here. No experimental data for n_0 are available yet in the metastable region. Recent measurements[21] of n_0 at high pressure in the stable region are in good agreement with our results (see Fig. 4). The dependence of n_0 with pressure can be fitted accurately with the empirical formula in the caption of Fig. 4, which allow us to estimate a pressure where n_0 would go to zero: $p_0 = 163 \pm 9$ atm.

The calculation of the excitation spectrum started from the evaluation of the intermediate scattering function $F(q,\tau) \propto \langle \psi_0 | e^{\tau \hat{H}} \hat{\rho}_{\vec{q}} e^{-\tau \hat{H}} \hat{\rho}_{-\vec{q}} | \psi_0 \rangle$, to be used as input of the GIFT method; the details of the method are given in Ref. [18]. In Fig. 5 we report the obtained $S(q,\omega)$ in the maxon region for several densities. It is evident that, in agreement with experiments, a well-defined maxon peak disappears at
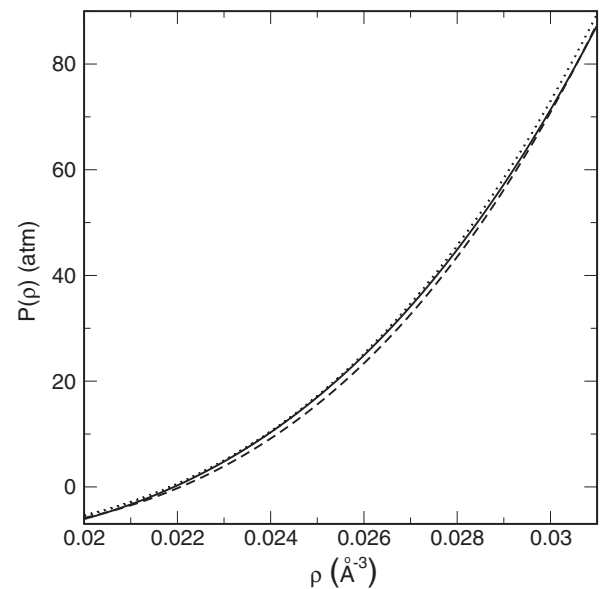

FIG. 3. Pressures in the liquid phase for the range of densities presently studied: (solid line) $P(\rho)$ as obtained from the equation of state with the interaction in Ref. [20]; (dashed line) $P(\rho)$ as obtained from the equation of state with the interaction in Ref. [19]; (dotted line) fit to experimental data (Ref. [27]).
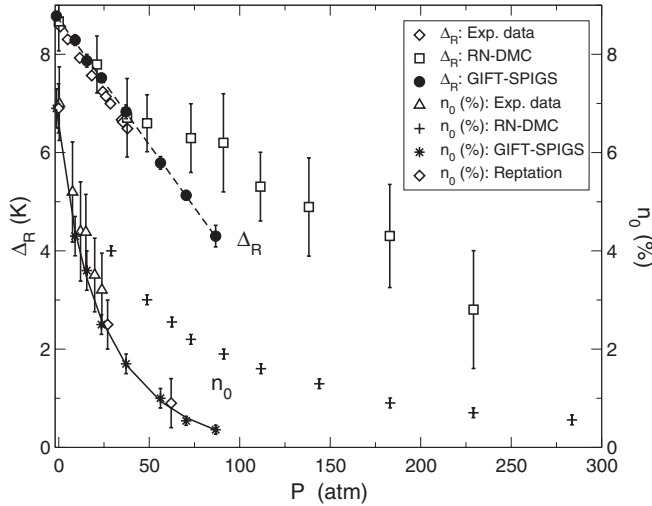
FIG. 4. Roton gap Δ_R and condensate fraction n_0 as a function of the pressure in the system compared with experimental data[8,21], with RN-DMC results[10] and reptation QMC results[9]; (dashed line) linear fit on SPIGS-GIFT results: $\Delta_R(P) = 8.71(2) \text{ K} - 0.0511(4) \text{ K/atm} \times P$; (solid line) fit on SPIGS results with the function $n_0(p) = \frac{n_0}{1+ap}(1 - p/p_0)^2$ with parameters: $n_0 = 0.0647(13)$, $p_0 = 163(9)$ atm, and $a = 0.035(4)$ atm^{-1}.

densities above freezing as observed in a recent neutron scattering experiment,[8] probably because its energy is higher than twice the roton one. At all densities $S(q,\omega)$ for a range of q around 2 Å^{-1} has a sharp peak and an additional broad peak at larger energies. The energy of the sharp peak has a minimum as function of q, that is, we find roton excitations at all densities, also in the metastable region. The roton excitation remains well defined in a wave vectors range compatible to that observed experimentally, above about 1.5 Å^{-1} and below 3 Å^{-1}. Above about 3 Å^{-1} the single-particle excitation peak
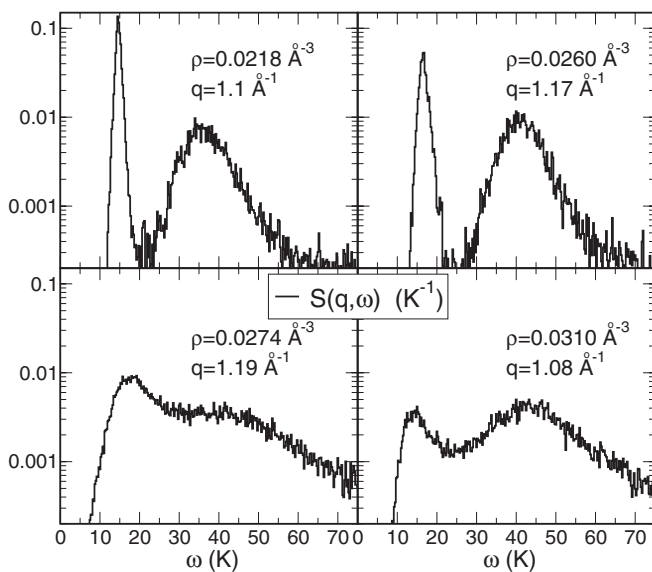

FIG. 5. GIFT[18] reconstructions of the dynamic structure factor $S(q,\omega)$ in the maxon region for different densities. Notice the logarithmic scale.
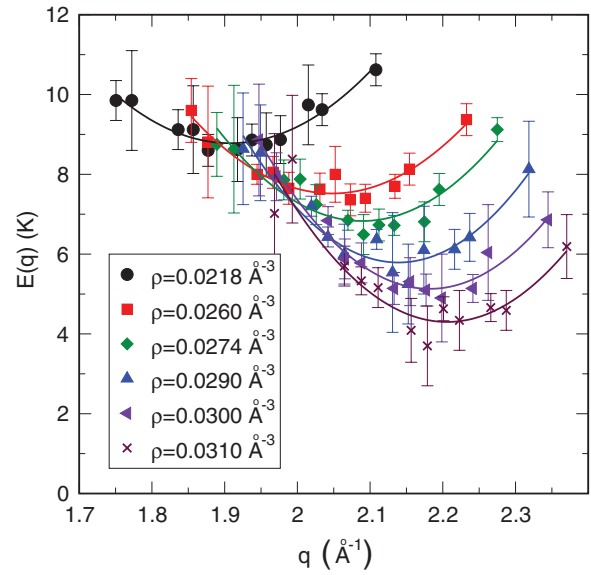

FIG. 6. (Color online) Excitation energies $E(q)$ as a function of the wave vector q in the roton region of the spectrum for different densities (see the legend). Solid lines represent a parabolic fit to the data with the standard formula: $E(q) = \Delta_R + \hbar^2(q - q_R)^2/2\mu_R$; the estimated parameters Δ_R, q_R, and μ_R are shown in Table I.

disappears from $S(q,\omega)$ leaving a broad contribution at all considered densities. In Fig. 6 the excitation spectrum $E(q)$ in a neighborhood of the roton minimum is shown for several densities (i.e., pressures); the statistical uncertainty has been assumed to be equal to the peak width.

The Landau parameters shown in Table I are obtained by a fit as explained in the caption of Fig. 6. The roton energy decreases at higher pressures and our results are in good agreement with experimental data that have been obtained up to a pressure of 40 bars by studying ^{4}He in Vycor.[8] Our results for the roton gap Δ_R as a function of pressure are shown in Fig. 4 and compared with the experimental data and the old RN-DMC estimation. Δ_R has a linear trend with pressure (see Fig. 4); this is true also for Δ_R computed with the interaction potential of Ref. 20, in this case Δ_R goes from 7.41(3) K [with $q_R = 2.04(1)$ Å^{-1}] near freezing to 4.23(12) K [with $q_R = 2.19(1)$ Å^{-1}] at about 89 atm. The pressure at which the linear trend would extrapolate to a zero roton energy computed with the potential in Refs. 19 and 20 turns out to be about 170 (168) atm, in agreement with the pressure extrapolated for a zero condensate fraction. This behavior is remarkably different from what was found from DMC calculations,[10] where a nonlinear trend has been observed; RN-DMC results gave a roton gap still greater than 2 K at a pressure of about 225 atm. Moreover, with our approach the roton energy can be extracted with quite higher accuracy.

A path integral simulation at finite temperature has given evidence for the existence of what has been called a superglass state.[11] We find no sign of such (super)glass phase in our simulations at $T = 0$ K and this could have consequence on the interpretation of the experiments related to the possible existence of a ^{4}He supersolid phase. Above $\rho = 0.031$ Å^{-3} our system readily starts a homogeneous nucleation process; at lower densities the system was found

to be a homogeneous and isotropic liquid with well defined roton excitations. We have tried to prevent nucleation in a number of ways, by modifying how configurations are sampled, or by changing the aspect ratio of the simulation box, or by changing the total imaginary projection time. In no case have we been able to avoid crystallization at ρ above 0.031 Å^{-3}.

The GIFT methodology also allows us to extract the single-quasiparticle strength $Z(q)$ from the estimated $S(q,\omega)$; in the roton region the peak is well defined, making an estimation of $Z(q)$ rather accurate. As far as we know, no data about $Z(q)$ exist for metastable phases in current literature; we plot our results in Fig. 1 . The relative strength of this peak, that is, $f(q) = Z(q)/S(q)$, evaluated at the roton wave vector turns out to be remarkably constant, around 75% at all densities of our computation.

IV. CONCLUSIONS

In conclusion, we have performed a microscopic study of the properties of overpressurized superfluid ^{4}He. In particular we have addressed the topic of the fate of the phonon-roton spectrum of the metastable system at zero temperature. We found remarkable agreement with experiments in the small range of metastable states experimentally explored up to now: the maxon peak disappears above freezing while the roton remains well defined up to the highest pressures. Roton energies have a linear trend with pressure and Δ_R extrapolates to zero at about 170 atm. This is in remarkable discrepancy with the results a previous QMC calculation.[10] No sign of a superglass[11] phase was observed; for pressures up to 87 atm the system behaves as a high density superfluid liquid, at higher pressures the system readily starts an homogeneous nucleation process.

[1] S. Balibar, Nature (London) **464**, 176 (2010).

[2] T. Schneider, R. Brout, H. Thomas, and J. Feder, Phys. Rev. Lett. **25**, 1423 (1970).

[3] T. Schneider, Phys. Rev. A **3**, 2145 (1971).

[4] T. Schneider and C. P. Enz, Phys. Rev. Lett. **27**, 1186 (1971).

[5] X. Chavanne, S. Balibar, and F. Caupin, Phys. Rev. Lett. **86**, 5506 (2001).

[6] H. Abe, F. Ogasawara, Y. Saitoh, T. Tatara, S. Kimura, R. Nomura, and Y. Okuda, Phys. Rev. B **71**, 214506 (2005).

[7] R. Ishiguro, F. Caupin, and S. Balibar, J. Low Temp. Phys. **148**, 645 (2007).

[8] J. V. Pearce, J. Bossy, H. Schober, H. R. Glyde, D. R. Daughton, and N. Mulders, Phys. Rev. Lett. **93**, 145303 (2004).

[9] S. Moroni and M. Boninsegni, J. Low Temp. Phys. **136**, 129 (2004).

[10] L. Vranjes, J. Boronat, J. Casulleras, and C. Cazorla, Phys. Rev. Lett. **95**, 145302 (2005).

[11] M. Boninsegni, N. V. Prokof'ev, and B. V. Svistunov, Phys. Rev. Lett. **96**, 105301 (2006).

[12] D. E. Galli and L. Reatto, Mol. Phys. **101**, 1697 (2003).

[13] D. E. Galli and L. Reatto, J. Low Temp. Phys. **134**, 121 (2004).

[14] M. Rossi, M. Nava, L. Reatto, and D. E. Galli, J. Chem. Phys. **131**, 154108 (2009).

[15] A. Sarsa, k.E. Schmidt and W. R. Magro, J. Chem. Phys. **113**, 1366 (2000).

[16] S. A. Vitiello, K. Runge, and M. H. Kalos, Phys. Rev. Lett. **60**, 1970 (1988).

[17] D. M. Ceperley, Rev. Mod. Phys. **67**, 279 (1995).

[18] E. Vitali, M. Rossi, L. Reatto, and D. E. Galli, Phys. Rev. B **82**, 174510 (2010).

[19] R. A. Aziz, F. R. W. McCourt, and C. C. K. Wong, Mol. Phys. **61**, 1487 (1987).

[20] R. A. Aziz, V. P. S. Nain, J. S. Carley, W. L. Taylor, and G. T. McConville, J. Chem. Phys. **70**, 4330 (1979).

[21] H. R. Glyde, S. O. Diallo, R. T. Azuah, O. Kirichek, and J. W. Taylor, Phys. Rev. B **83**, 100507(R) (2011).

[22] W. Lechner and C. Dellago, J. Chem. Phys. **129**, 114707 (2008).

[23] O. H. Nielsen and R. M. Martin, Phys. Rev. B **32**, 3780 (1985).

[24] J. Boronat and J. Casulleras, Phys. Rev. B **49**, 8920 (1994).

[25] S. Moroni, D. E. Galli, S. Fantoni, and L. Reatto, Phys. Rev. B **58**, 909 (1998).

[26] E. Tanaka, K. Hatakeyama, S. Noma, and T. Satoh, Cryogenics **40**, 365 (2000).

[27] F. Caupin, J. Boronat, and K. H. Andersen, J. Low Temp. Phys. **152**, 108 (2008).

[28] M. Boninsegni, N. Prokof'ev, and B. Svistunov, Phys. Rev. Lett. **96**, 070601 (2006).

[29] R. Rota and J. Boronat, J. Low Temp. Phys. **166**, 21 (2012).